Electronic Supplementary Material (ESI) for Materials Advances.

Supporting Information

Oxygen vacancies in oxidized and reduced vertically aligned *α*-MoO_3 nanoblades

Sohaila Z. Noby,*[1,2] Azhar Fakharuddin,[1] Stefan Schupp,[1] Muhammed Sultan,[3] Marina Krumova,[4] Malte Drescher,[4] Mykhailo Azarkh,[4] Klaus Boldt,[5] Lukas Schmidt-Mende*[1]

[1]Department of Physics, University of Konstanz, 78467 Konstanz, Germany

[2]Department of Solid-state Physics, National Research Centre (NRC), 12622 Cairo, Egypt

[3]Nanoscience and Technology Department, National Centre for Physics, 440000 Islamabad, Pakistan

[4]Department of Chemistry, University of Konstanz, 78467 Konstanz, Germany

[5]Department of Chemistry & Zukunftskolleg, University of Konstanz, 78467 Konstanz, Germany

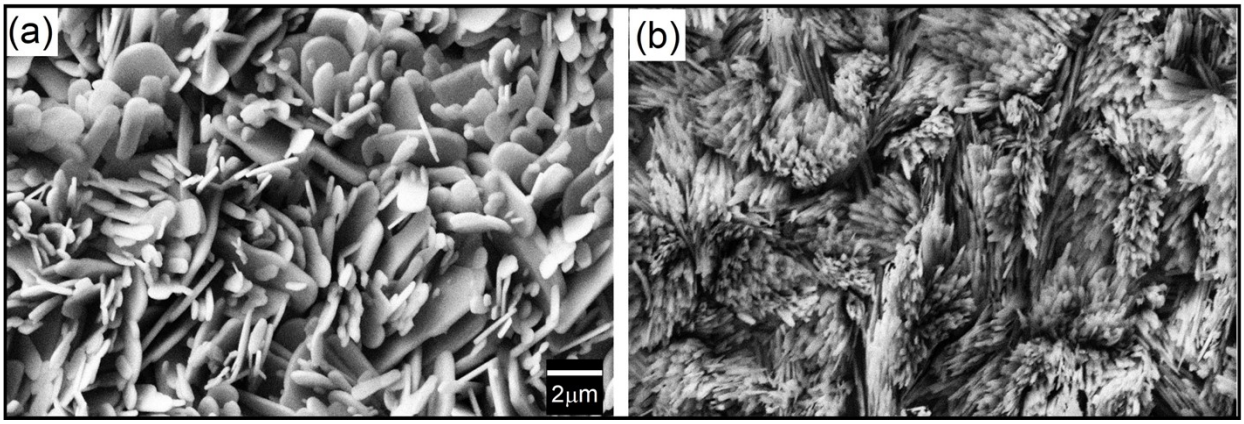

Fig. S1: (a-b) FE-SEM micrographs of vertically aligned α-MoO_3 nanoblades annealed under N_2 and vacuum conditions at 500˚C, respectively.

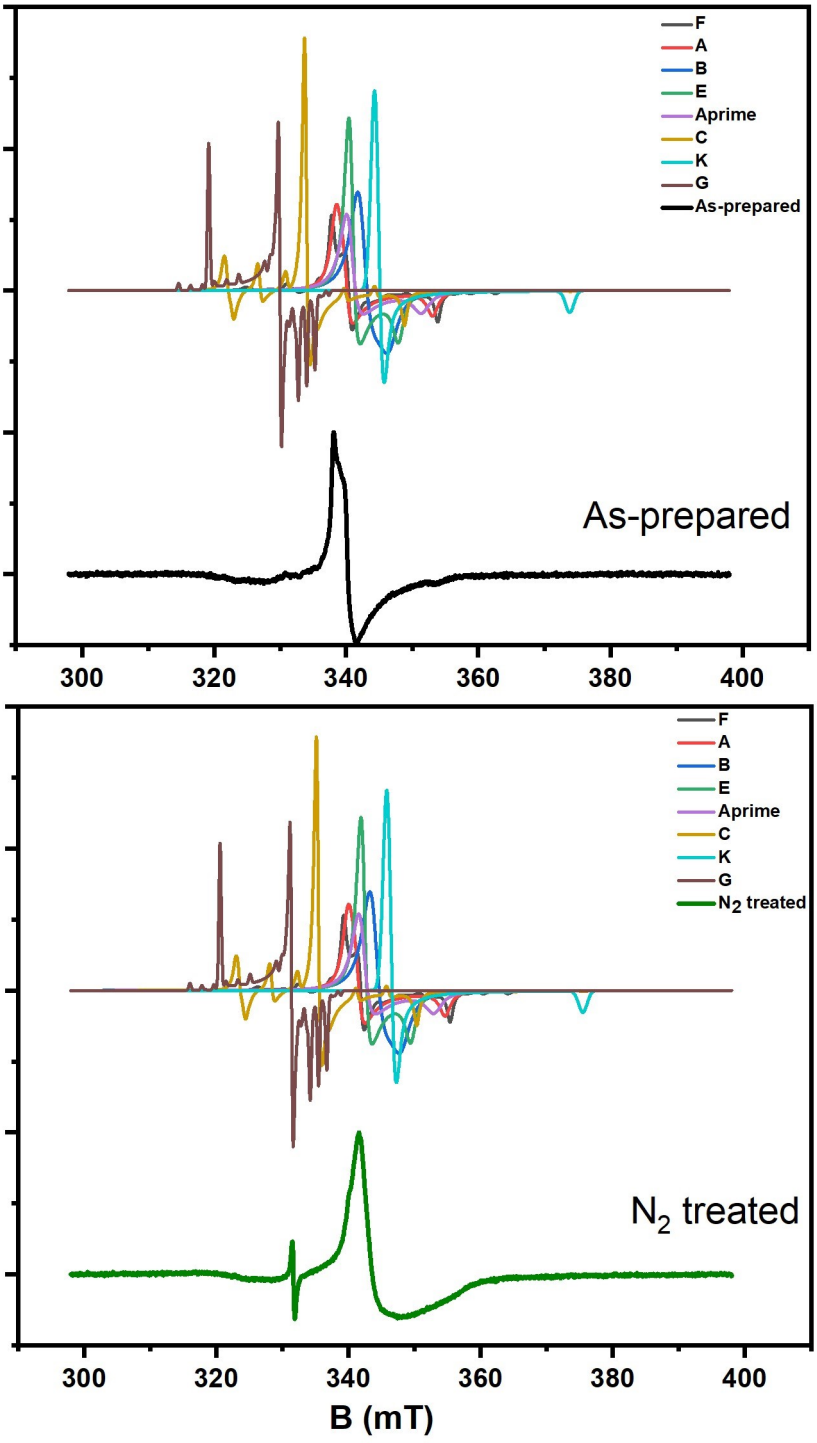

Fig. S2: EPR spectra of as-prepared -MoO_3 nanoblades, nanoblades treated under N_2 atmosphere, and corresponding component signals given previously for reduced α-MoO_3.[1, 2]

A set of EPR spectra Fig. S2 that correspond to known Mo^{5+} species was generated and compared to the experimental EPR spectra as can be seen in supporting information (Fig. S2). The spectral components A, À, B, F, and E were given by K. Dyrek *et al*.[2] They can be found in distorted octahedral MoO_6 oriented as hexacoordinate, rhombically, and pentacoordinate of rhombic symmetry by removing weak oxygen atoms from Mo-O bonds. The spectral components K, C, and G were eliminated from further analysis because they contain signals outside the range of the experimental spectrum. The spectral component B was found to have a minor contribution to the spectra of N_2 and H_2 treated samples and can be completely neglected in the spectra of as-prepared and vacuum treated types. Thus, the corresponding types of defects are not significant in the α-MoO_3 nanoblades as well. Unfortunately, a detailed simulation of experimental spectra with the remaining components was not possible because the exact line shape of the individual components is not known. However, it is possible to conclude that α-MoO_3 nanoblades are heterogeneous samples that contain several Mo^{5+} based defects.

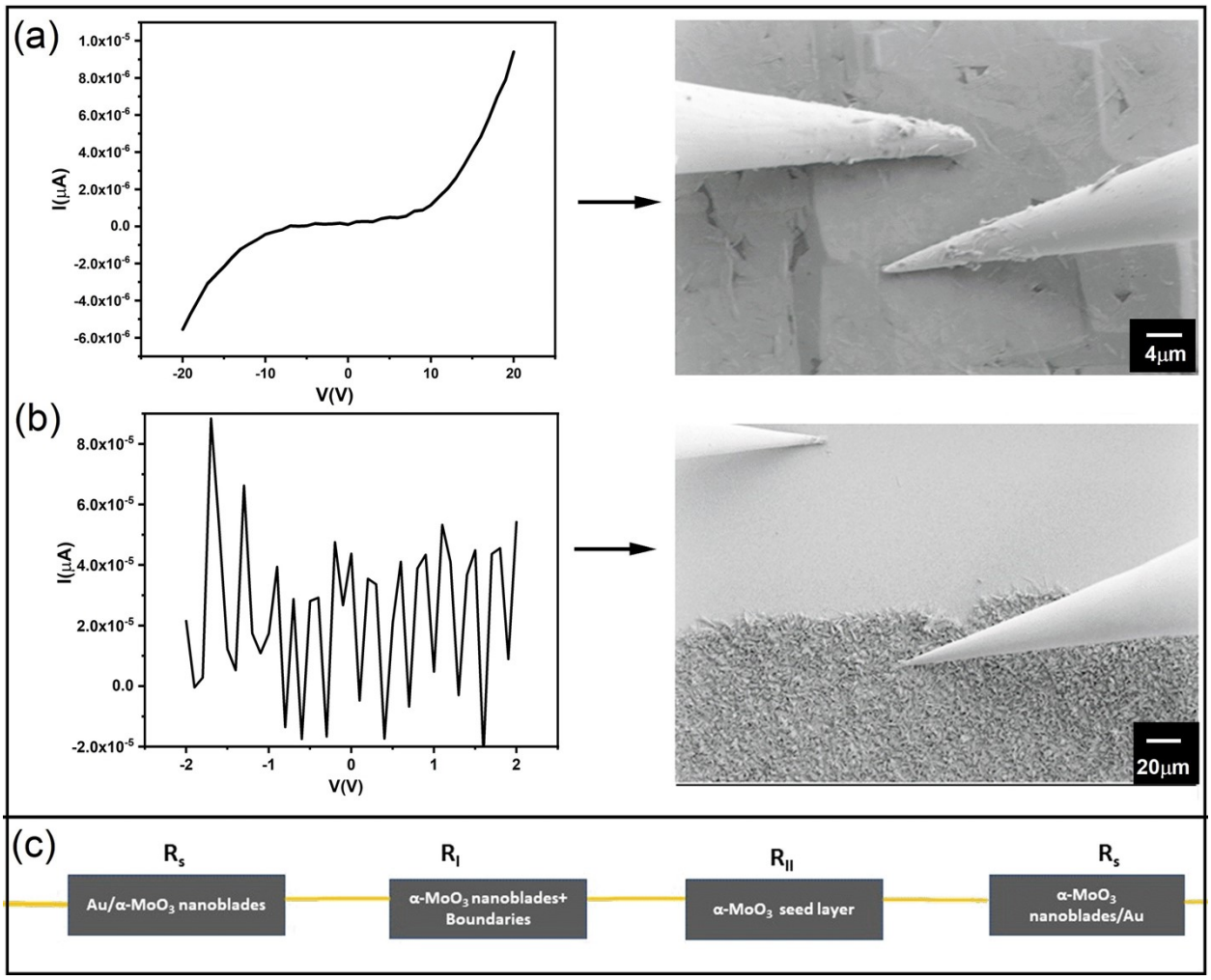

Fig. S3: a) Room-temperature I-V characteristic at room-temperature of the seed layer of 10 nm/100 nm of Cr/MoO_3 on Si/SiO_2 substrates with indication of the measured device FE-SEM micrograph. (b) I-V characteristic of vertically aligned α-MoO_3 nanoblades as top-bottom electrode configuration through the seed layer on Si/SiO_2 substrates with indication of the measured device FE-SEM micrograph. (c) The supposed total resistance of the electrical device.

We supposed that there are two possible electric pathways: One pathway is across the interconnected nanoblades and the nanoblades to the seed layer, and then again through the nanoblades to the second terminal electrode (see Fig. 4d). To clarify the contribution of the seed layer, a fast electrical measurement has been performed using a nanoprobing system, since the seed layer suffers from pin-holes (cannot use FTO) in addition to the Cr layer as an island-like morphology, which has reported in our previous study.[3] Fig. S3a shows the I-V characteristic of the seed layer on Si/SiO_2 wafer, which indicates an almost insulating behaviour of this layer at

room temperature. This result is consistent with the nature of the air treated α-MoO_3 as insulator layer.[4, 5] Additionally, the Cr layer is not a compact layer but rather contains islands-like morphology. Moreover, as is given in Fig. S3 (b), hardly any current flows from the top of the vertically aligned α-MoO_3 though the seed layer. Subsequently, the device resistance can be simplified as shown in Fig. S3-(c) Here, the total resistance is a series of resistances: Two metal contacts to the vertically aligned α-MoO3 nanoblades, the boundaries between the nanoblades themselves, and barely the seed layer contributing to the current flow. Temperature dependent I-V characteristics have been recorded and plotted on a semi-logarithmic scale in Fig. S4(a-e). The semi-logarithmic temperature dependent I-V curves show nonlinearity and symmetric trends in both forward and reverse bias. This behavior suggests the formation of a lower Schottky barrier at the interfaces between the metal electrode and the nanoblades (Au/α-MoO_3/Au diode).[6, 7]

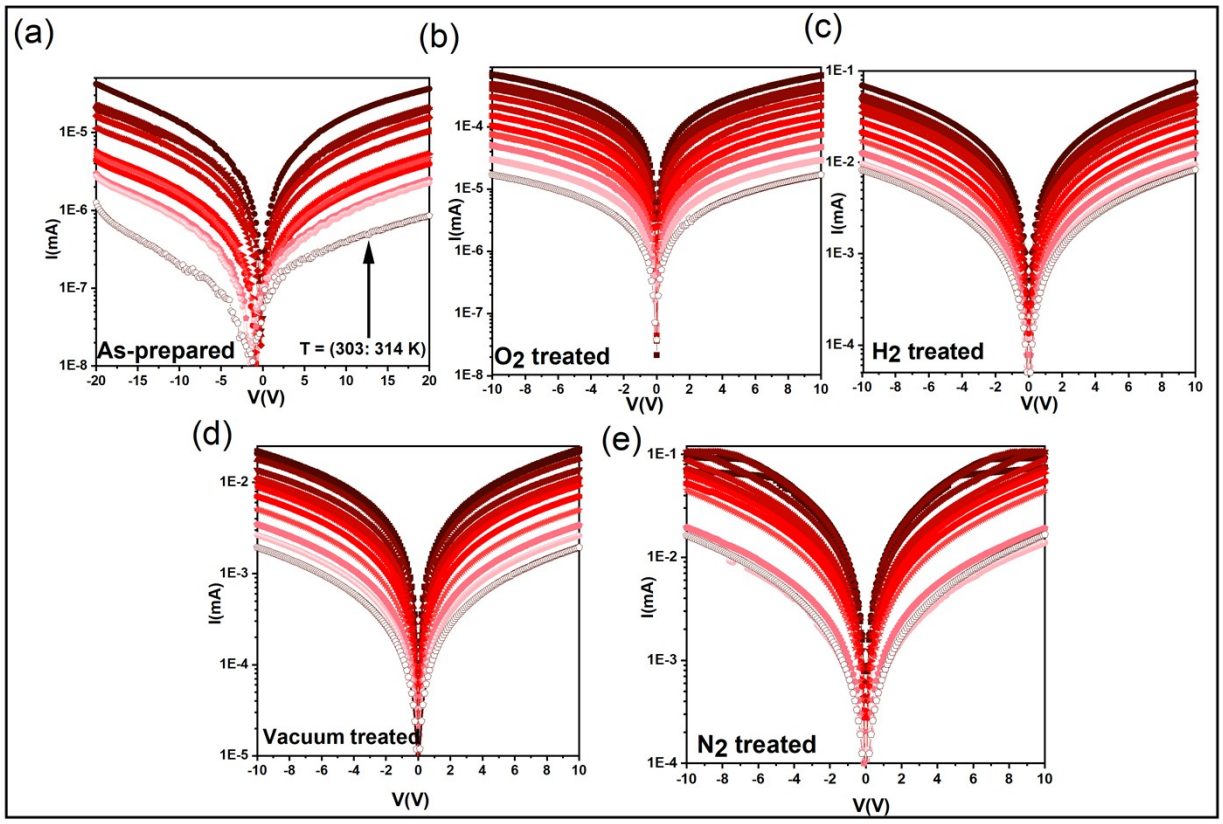

Fig. S4: (a-e) Temperature dependent semi-logarithmic I-V characteristics (30-130°C)of as-prepared vertically aligned α-MoO_3 nanoblades and vertically aligned nanoblades on FTO substrates treated under O_2, H_2, vacuum, N_2 atmospheres, respectively.

Table. S 1 The estimated values of the product values of color center concentration *N* and oscillator strength f for as-prepared vertically aligned α-MoO_3 nanoblades on FTO substrates, and for films treated under oxidizing and reducing conditions.

Sample	Band-1 (cm^{-3})	Band-2 (cm^{-3})
As-prepared	$(1.07\pm0.93)\times10^{20}$	$(3.89\pm3.67)\times10^{21}$
O2 treated	$(3.00\pm2.88)\times10^{20}$	$(7.79\pm9.78)\times10^{20}$
H2 treated	$(3.26\pm0.69)\times10^{20}$	$(2.43\pm0.21)\times10^{21}$
Vacuum treated	$(2.25\pm0.79)\times10^{20}$	$(7.25\pm5.73)\times10^{20}$
N2 treated	$(3.12\pm0.18)\times10^{20}$	$(1.17\pm0.21)\times10^{21}$

X-ray photoelectron spectroscopy analysis

X-ray photoelectron spectroscopy (XPS) was used for identifying the surface stoichiometry of oxidized and reduced vertically aligned α-MoO_3 as is shown in Fig. S5. The doublet peaks around 235.6 and 232.5 eV are attributed to the binding energies of 3d3/2 and 3d5/2 orbitals of Mo^{6+}, with an energy of spin-orbital splitting of 3.15 eV that is typical for α-MoO_3.[8, 9] The interfacial reduction of Mo^{6+} and Mo^{5+} at binding energies of 231.2 and 234.35 eV can be seen in XPS spectra for oxidized and reduced α-MoO_3 nanoblades, and they correlate to the existence of oxygen vacancies even in the case of oxidized α-MoO_3.[10, 11] These findings further confirm our observations, obtained by electronic measurements, of the presence of shallow level in α-MoO_3 nanoblades even under an oxygen rich atmosphere. They are in a good agreement with the theoretical calculation by Guo *et al*.[12] It is worth to mention that in vacuum treated samples, there is a slight shift of the peaks to a higher binding energy by ≈0.2 eV. This can be related to the position of the Fermi level and defects.[12] Moreover, pre-exposure to air gives additional components, which are included to the deficiency and produce uncertainty ratios of the reduced Mo ions to Mo^{6+}. (XPS is a surface sensitive method.) Additionally, the concentrations of reduced oxidation states are below the detection limit of XPS[9] (lower concentration). Appearance of different oxidation states is consistent with our observation of altering the electronic properties as a proof of existence of oxygen vacancies even in oxidized α-MoO_3. Furthermore, it is demonstrated that in near-stoichiometric α-MoO_3 the concentration of oxygen vacancies cannot be determined accurately using XPS. Formation of reduced ions releases free electrons, which become delocalized in the layers and act as Drude model like free electrons.[11, 13] Mo^{5+} oxidation states are found to be related to the loss of oxygen, which is associated to octahedral MoO_3 within the bilayer in the (x,z) plane as has been given previously.[14] Careful observation of the vacuum treated sample shown in Fig.

S6 shows a lower intensity in the deconvolution corresponds to Mo^{5+} than the intensities for the other α-MoO_3 samples reduced under H_2 and N_2. An explanation for this is that the material is solely reduced to Mo^{5+} under the vacuum condition.[14] The existence of oxygen vacancies can be further seen from O1s spectra in Fig. S6. The deconvolution can be seen as around 530.8 and 531.7 eV corresponding to Mo-O and Mo-OH, respectively, without observation of water vapor formation, which has been seen even in oxidized α-MoO_3 in previous studies.[15] The hydroxyl components can result from the existence of ionized oxygen species O^{2-} or O^-, where O^- is the dominant ion, and which can have a similar binding energy as lattice oxygen found in our binding energy range.[16, 17] This has been pointed out using EPR measurements. No observation of the transition to MoO_2 was observed for all conditions, and even no bronze molybdenum oxide (H_xMoO_{3-x}) was formed in this range of applied thermal treatment. As has been demonstrated in the literature, 500˚C is considered as the transition temperature to obtain metallic molybdenum oxide (MoO_2).[14] Additionally, a longer time is needed to obtain bronze molybdenum oxide.[18] This observation ties very well with prior research showing that in the initial step of reducing α-MoO_3, formation of Mo^{5+} introduces a lattice rearrangement of the corner to edge-sharing oxygen in the octahedral structure in the lattice.[14] In the N_2 treated nanoblades, no prominent peaks can be found for a binding energy corresponding to attached N (at 398.5 eV) [19]in the survey spectrum presented in Fig. S6, which is identical with that of α-MoO_3.[20] This can be attributed to the interaction between nitrogen and lattice oxygen and the according release of NO or NO_2 gases, which can be seen as a formation of Mo^{5+} cations in the octahedral structure.

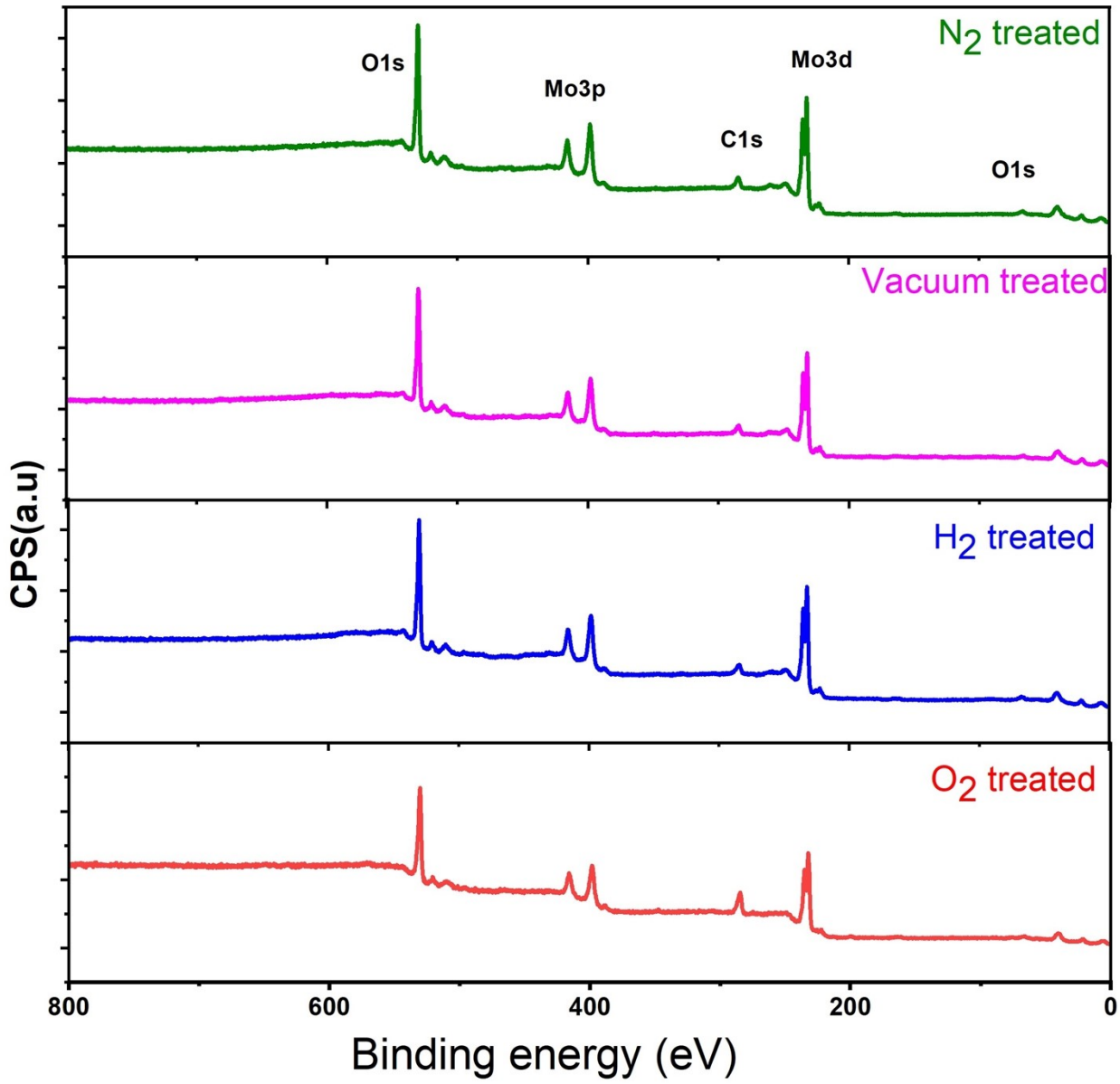

Fig. S5: XPS spectra survey of α-MoO_3 vertically aligned nanoblades treated under O_2, H_2, vacuum and N_2 atmospheres, respectively.

.

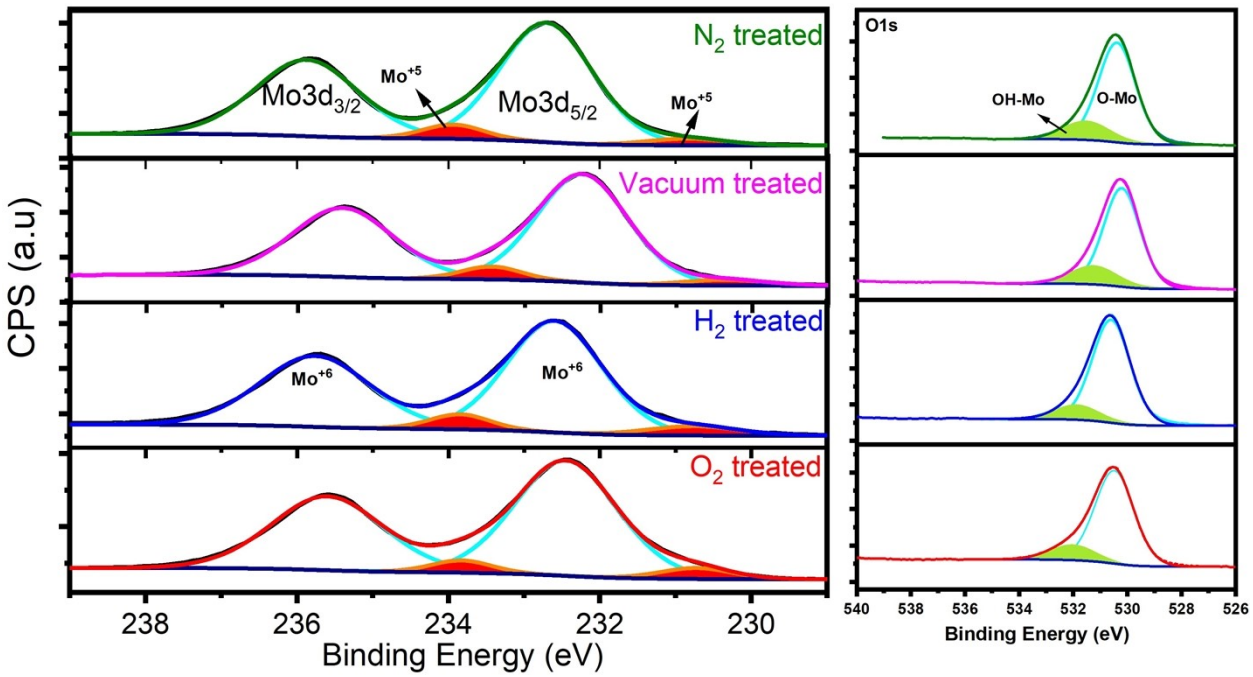

Fig. S6: XPS spectra of O1s and Mo3d of α-MoO_3 vertically aligned nanoblades treated under O_2, H_2, vacuum and N_2 atmospheres, with indication of deconvolution peaks corresponding to Mo^{6+} and Mo^{+} in Mo3d, as well as O-Mo, OH-Mo for O1s core levels.

1. M. Łabanowska, *Physical Chemistry Chemical Physics*, 1999, **1**, 5385-5392.
2. K. Dyrek and M. Labanowska, *J Chem Soc Faraday T*, 1991, **87**, 1003-1009.
3. S. Z. Noby, K. K. Wong, A. Ramadoss, S. Siroky, M. Hagner, K. Boldt and L. Schmidt-Mende, *RSC Advances*, 2020, **10**, 24119-24126.
4. C. Julien, A. Khelfa, O. M. Hussain and G. A. Nazri, *Journal of Crystal Growth*, 1995, **156**, 235-244.
5. V. Nirupama, K. R. Gunasekhar, B. Sreedhar and S. Uthanna, *Current Applied Physics*, 2010, **10**, 272-278.
6. R. K. Gupta, K. Ghosh and P. K. Kahol, *Physica E: Low-dimensional Systems and Nanostructures*, 2010, **42**, 1509-1512.
7. H. M. Chenari, H. Sedghi, M. Talebian, M. M. Golzan and A. Hassanzadeh, *Journal of Nanomaterials*, 2011, **2011**, 1-4.
8. S. Guimond, D. Göbke, J. M. Sturm, Y. Romanyshyn, H. Kuhlenbeck, M. Cavalleri and H. J. Freund, *The Journal of Physical Chemistry C*, 2013, **117**, 8746-8757.
9. J. Baltrusaitis, B. Mendoza-Sanchez, V. Fernandez, R. Veenstra, N. Dukstiene, A. Roberts and N. Fairley, *Applied Surface Science*, 2015, **326**, 151-161.
10. *Nanoscale*, 2014, **6**, 13882.
11. M. M. Y. A. Alsaif, A. F. Chrimes, T. Daeneke, S. Balendhran, D. O. Bellisario, Y. Son, M. R. Field, W. Zhang, H. Nili, E. P. Nguyen, K. Latham, J. van Embden, M. S. Strano, J. Z. Ou and K. Kalantar-zadeh, *Advanced Functional Materials*, 2016, **26**, 91-100.
12. Y. Guo and J. Robertson, *Applied Physics Letters*, 2014, **105**.

13. R. S. Datta, F. Haque, M. Mohiuddin, B. J. Carey, N. Syed, A. Zavabeti, B. Zhang, H. Khan, K. J. Berean, J. Z. Ou, N. Mahmood, T. Daeneke and K. Kalantar-zadeh, *Journal of Materials Chemistry A*, 2017, **5**, 24223-24231.
14. P. A. Spevack and N. S. Mcintyre, *J Phys Chem-Us*, 1992, **96**, 9029-9035.
15. Y. Zhen, J. Wang, F. Fu, W. Fu and Y. Liang, *Nanomaterials (Basel)*, 2019, **9**.
16. J.-C. Dupin, D. Gonbeau, P. Vinatier and A. Levasseur, *Physical Chemistry Chemical Physics*, 2000, **2**, 1319-1324.
17. T. G. G. Maffeis, M. W. Penny, A. Castaing, O. J. Guy and S. P. Wilks, *Surface Science*, 2012, **606**, 99-103.
18. D. J. Goyal, C. Agashe, M. G. Takwale and V. G. Bhide, *Journal of Crystal Growth*, 1993, **130**, 567-570.
19. S. A. Khalate, R. S. Kate, H. M. Pathan and R. J. Deokate, *Journal of Solid State Electrochemistry*, 2017, **21**, 2737-2746.
20. J. Yang, X. Xiao, P. Chen, K. Zhu, K. Cheng, K. Ye, G. Wang, D. Cao and J. Yan, *Nano Energy*, 2019, **58**, 455-465.